



Evaluation of a weather forecasting model and HEC-HMS for flood forecasting: case study of Talesh catchment

Mohammad Reza Goodarzi¹ · Mohammad Javad Poorattar¹ · Majid Vazirian¹ · Ali Talebi²

Received: 22 October 2023 / Accepted: 7 December 2023 / Published online: 28 January 2024
© The Author(s) 2024

Abstract

Reports demonstrate that floods are among the most prevalent and deadliest natural disasters affecting 520 million people annually. The present study seeks to evaluate flood forecasting using the weather research and forecasting (WRF) model and the Hydrologic Engineering Center-Hydrologic Modeling System (HEC-HMS) model. To this end, WRF and HEC-HMS were calibrated by comparing their results with the data observed at measuring stations. Then, the output rainfall data of the WRF model were implemented by the calibrated HEC-HMS model and were examined using the statistical indices, which were revealed to be 4.13, 3.42, and 2.67 for the flow volume and 6.2, 2.46, and 5.11 for the peak flow, suggesting the accurate performance of WRF model alongside HEC-HMS in the Talesh catchment.

Keywords Flood risk · Weather forecasting · WRF · HEC-HMS · Rainfall · Runoff

Introduction

Among all natural hazards capable of causing catastrophes, floods are the most prevalent ones that cause suffering to humans and extensive damage to buildings, infrastructures, crops, etc. World Water and Environmental Engineering Journal (London) has thus declared water to be the origin of half of natural disasters (Gore and Petts 1989). The persistence of the flood phenomenon would leave irreparable damage to the soil and water resources of a country. Hence, understanding the factors and parameters involved in floods is of vital prominence in controlling and mitigating this phenomenon. In other words, one would have to explore the

behaviors of processes involved in flood before making any plans to control it (Singh et al. 2021; Kaya and Derin 2023).

In California, Anderson et al. used the MM5 model and forecasting data from the Eta model, and a rainfall calibrated with the prediction resulting from a mesoscale MM5 model and 48-h forecasting periods to simulate rainfall. The HEC-HMS model was then calibrated using rainfall, time, and runoff hydrograph and implemented with MM5 rainfall forecasting data. The automation of this process brought about an invaluable reservoir management tool. The outputs of HEC-HMS calibrated for the same thunder were thus consistent with forecasting data from HEC-HMS and MM5 models in terms of flow and effluent peak time (Anderson et al. 2002).

Weisman et al. (2008) presented an account of previous practices performing 36-h cumulus forecasts (4km resolution) using the advanced weather research and forecasting (WRF-ARW) over the springs and summers of 2003–2005 in the USA and compared the forecasts with operational 12km data from the Eta model. Their results suggested that land surface, microphysics, resolution, and PBL schemes played a more vital role than forecasting errors, indicating the need for further research to document the sources of such errors at these time scales. Moreover, their results indicated that a systematic orientation was also needed for the PBL scheme (YSU) emphasizing the need for persistent modification of

✉ Mohammad Reza Goodarzi
Goodarzimr@yazd.ac.ir

Mohammad Javad Poorattar
mohaattar1997@gmail.com

Majid Vazirian
vazirian.majid@gmail.com

Ali Talebi
talebisf@yazd.ac.ir

¹ Department of Civil Engineering, Yazd University, Yazd, Iran

² Faculty of Natural Resources, Yazd University, Yazd, Iran

the physics of packages for practical forecasting (Weisman et al. 2008).

In the USA, Gilliam and Pliem performed a study in 2009 by using the Pleim-Xiu land surface scheme, Pliem land surface scheme, and asymmetrical cumulus model (version 2) to compare the simulations made using the new physics of the WRF model, simulations generated by the MM5 model, and other WRF configurations. Results of their analyses revealed that in summer simulation, smaller errors were observed in the WRF simulation model that uses a new physics compared to the configuration similar to MM5 across the whole domain. However, this simulation model is as generally inaccurate as others in winter although it indicated a good performance at temperature categories under 2m (Pleim and Gilliam 2009).

Zhang et al. (2011) used advanced weather research and forecasting (WRF-ARW) to enhance the demonstration and simulation of the modified boundary level (MBL) clouds over Southeast Pacific (SEP) for a whole month of October in southeast Pacific. They employed the National Centers for Environmental Prediction Global Forecast System (NCEP (NFL)) as initial, lateral, and boundary conditions and observational sea surface temperature (SST) and compared the results with satellite observations. Results indicated that the modified Tiedtke scheme successfully captures the MBL structure's main features and the model managed to simulate the large-scale atmospheric circulation in the eastern Pacific reasonably.

Roy et al. (2013) used US Hydrological Engineering Center's Hydrologic Modeling System (HEC-HMS) (employing the soil moisture accounting algorithm—SMA) in hydrological forecasting of the Subarnarkha River, east India. Their results suggested the model's accurate performance in simulating the current and, consecutively, water quantification. Moreover, using semi-annual parameter sets accounting for changes was revealed to have improved the model's hydrological performance (Roy et al. 2013).

Nasiri and Talebi (2020) used the HEC-HMS software to rank the sub-basins in Chenarsukhteh watershed, Iran, with an area of 141.591 km² in terms of flood risk. This study assessed the impacts of flood risk using the two physical criteria of flow volume and current peak discharge as the parameters involved in a flood. As a result, flood hydrographs corresponding to rainfall were calculated for all sub-basins and each hydrograph's extent of influence was obtained in output flood generation by sequential sub-basin elimination, allowing the classification of the sub-basins in terms of the flood risk level.

Goodarzi et al. used WEF resources for sustainable city development for future climate change. Two scenarios Rcp2.6 and Rcp8.5 from the fifth IPCC assessment report with the output of HADGEM2 model were used for the city of Borujerd, Iran. The urban morphological dataset was used via

ArcGIS and demonstrated that in the next period, the amount of precipitation will change 20 to 40 percent (Goodarzi et al. 2022a, b).

In Ethiopia, Tedla et al. (2022) examined the WRF model's rainfall forecasting accuracy in a catchment, with results indicating a high forecasting accuracy for 1–3-day rainfall forecasting periods while the accuracy would drop for periods of 4–5 days. The model was also revealed to be more accurate in simulating light rains (less than 6mm daily) than medium and heavy rains (over 6mm daily) (Tedla et al. 2022).

In Spain, Merino et al. (2022) investigated used the weather research and forecasting (WRF) model to investigate hourly precipitation for 45 extreme precipitation events (EPEs) using two planetary boundary layers (PBLs) and microphysics schemes. Their results indicated that the microphysics scheme was more accurate than the planetary boundary layers (PBLs) (Merino et al. 2022). This is very important to choose the basin that has the most locations of rain gauge and hydrometer stations, although in ungauged basins, geostatistical methods can also be used to measure mistaken data (Goodarzi and Vazirian 2023).

The recurrent incidence of floods in Talesh catchment (north of Iran) and its resulting human casualties, financial damages, and loss of amenities such as power, water, etc., in this region highlights the importance of examining various flood forecasting and control methods that are being widely used in practice across the globe to save lives and prevent damage to properties in this region. On the other hand, meteorological models must be used alongside hydrological models to study floods given that meteorological factors play an extremely prominent role in the occurrence of floods, i.e., no heavy flood would occur unless heavy precipitation happens. Thus, the present study integrates a mesoscale weather research and forecasting (WRF) model with an HEC-HMS hydrological model, hence examining a hydrodynamic model to forecast flood in the Talesh catchment area. Moreover, this study examines the results of WRF and HEC-HMS models' integration and analyzes the spatial distribution of rainfall effective in floods in Talesh catchment given the research gap in terms of the spatial distribution of rainfalls contributing to flooding, which is a significant parameter in forecasting flood—especially in river banks. For this purpose, WRF and HEC-HMS models were first calibrated with rainfall data from the WRF model, and the resulting output was used by HEC-HMS to predict floods. The output of the WRF model alongside HEC-HMS would eventually be assessed using hydrometric data (Fig. 1).

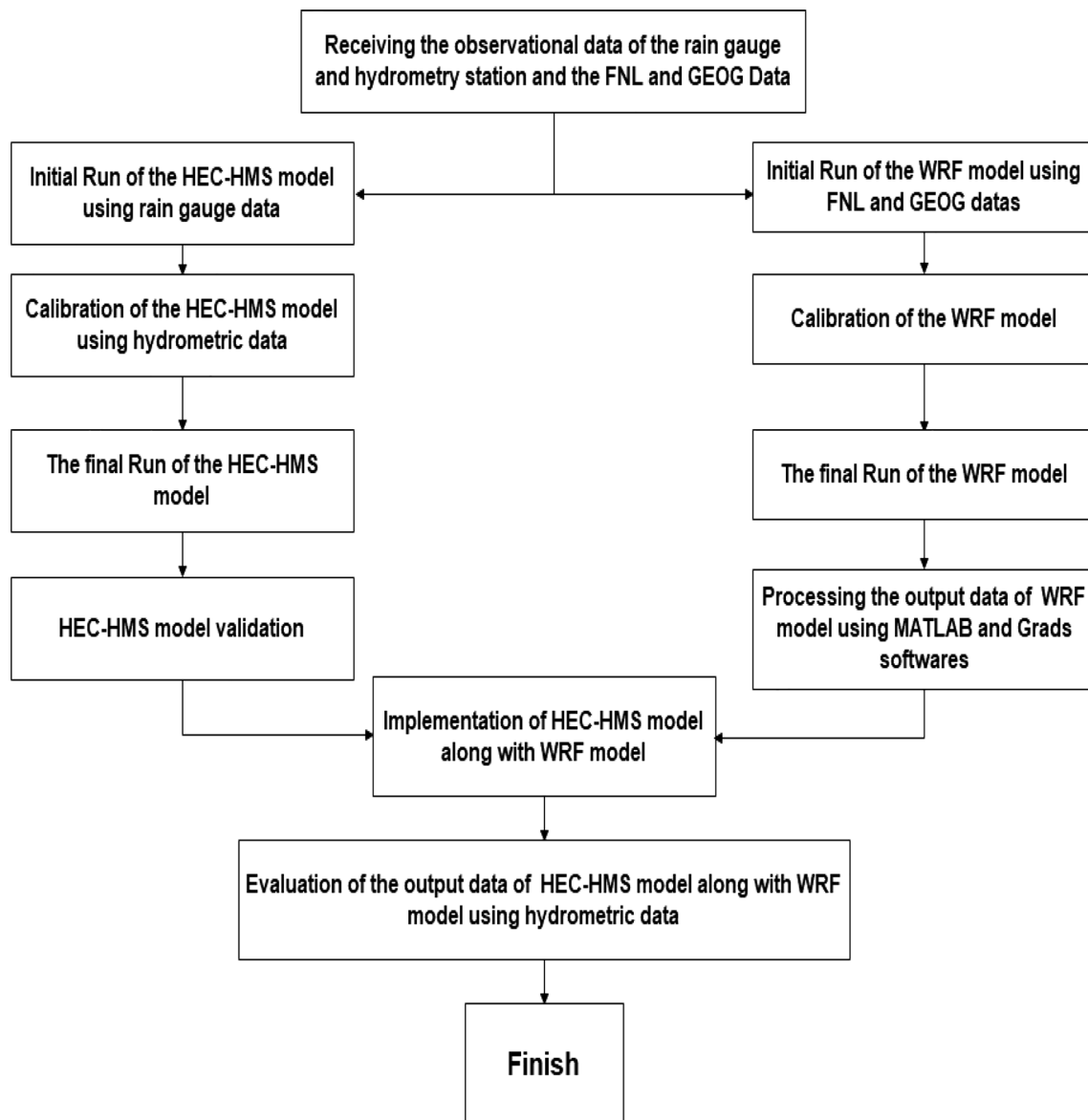


Fig. 1 Research method flowchart

Materials and methods

Study area

Situated between Aras and Sefidroud catchments, the basin area of Talesh rivers is among the sub-basins of the Caspian Sea with an area of 685,378 hectares and is among the rainiest sub-basins in Iran. The noteworthy point regarding the Talesh catchment is the multitude of rivers in it, which complicates hydrological modeling in the area. The northernmost river in the catchment that had the most position concerning rain gauge and hydrometer stations was thus selected as the studied river (Fig. 2).

Figure 3 indicates an illustration of the flood that occurred in the first peak of the studied period in Talesh County as an example,

Data

The present study used observational data obtained from Talesh rain gauge station and Safar Mahalleh Hydrometer stations as indicated in Table 1 For this purpose, six-hour precipitation data from Talesh stations and daily discharge data from Safar Mahalleh hydrometer station were obtained from Gilan Province's Regional Water and Meteorology Department for six months from September 23, 2018, until March 21, 2019.

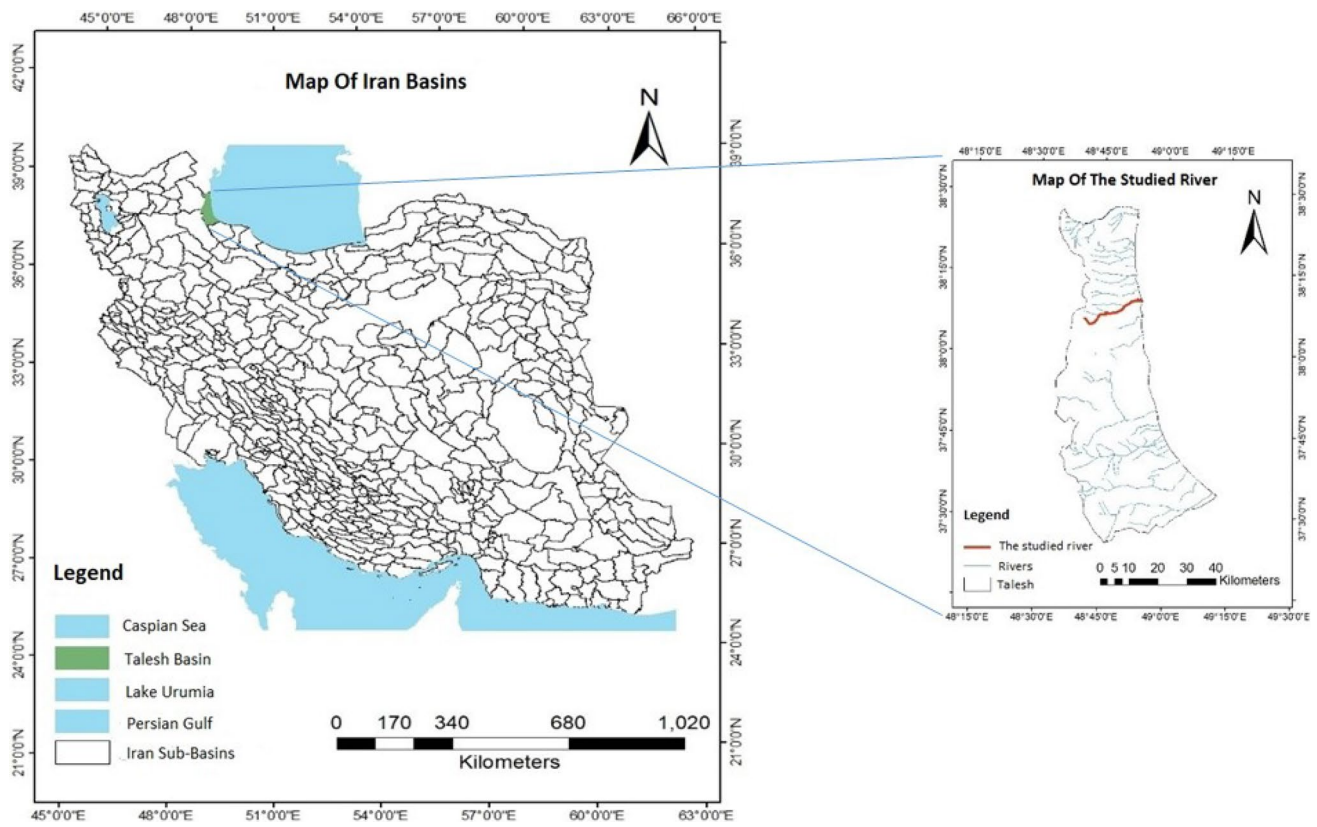


Fig. 2 The studied river situated in the Talesh basin in Iran



Fig. 3 Talesh flood on 09/27/2018

Table 1 Talesh stations specifications

No	Station	Station type	Established year	Above sea Level (m)	Latitude (°E)	Longitude (°N)
1	Talesh	Rain gauge	2000	7	38.19	48.54
2	Safar mahale	Hydrometry	1993	50	38.15	48.84

Moreover, FNL input data were used at a 0.25 resolution to implement the un-grid section in WRF model preprocessing. The FNL data are NCEP data reprocessed by the Air Resource Laboratory affiliated with NOAA. These data are available with a 1° horizontal resolution for 26 pressure levels (0111–011 hectopascal) and with a six-hour time step from July 1999. NCEP's final global-scale operational analyzed data (FNL for short) use the Global Data Integration System (GDAS) to acquire the initial input data for the system.

The GDAS system collects observational data from across the globe using the GTS2 global telecommunication system. NFL data are ultimately generated similarly to the model used by the National Centers for Environmental Prediction (NCEP) to generate Global Forecasting System (GFS) data (McQueen et al. 1997).

Furthermore, global geographic data were used to implement the geogrid portion of the WRF model preprocessing. These data contain land surface data read on a simple plane with a binary format.

WRF model introduction

Numerical weather prediction (NWP) models are numerical models developed based on basic physics and fluid equations and used to forecast oceanic and atmospheric conditions. A wide variety of numerical models have been introduced to be employed at regional and global scales in different countries of the world so far seeking to forecast atmospheric conditions. The weather research and forecasting model (WRF) is known to be among the most efficient and best of these numerical models.

Developing a weather research and forecasting (WRF) model is a multi-organizational effort aimed at the introduction of a next-generation mesoscale forecasting data assimilation system capable of helping both understand and forecast the weather at mesoscale and accelerate research operations. This model is a shared effort between NCAT and the Mesoscale and Microscale Meteorology (MMM) Laboratory, National Centers for Environmental Prediction (NCEP), National Oceanic and Atmospheric Administration (NOAA), the Forecasting System Laboratory (FSL), Air Force Weather Agency (AFWA), the Naval Research Laboratory (NRL), Center for Analysis and Prediction of Storms (CAPS) at the University of Oklahoma, and the Federal Aviation Administration (FAA) alongside several academic scientists (Skamarock et al. 2008).

The WRF model runs under Linux with Hdf5, Netcdf, Libpng, Jasper, Mpich, and Netcdf-Fortran as the most important packages for its implementation. The advanced WRF code contains several preliminary executables (ideal.exe, real.exe), a numerical integration (wrf.exe), and a one-way nesting program (ndown.exe). Meteorological

data and data on land features are prepared in the pre-processing system (WPS) as initial forecasts. This model is non-hydrostatic (although featuring a hydrostatic option) with an Arca C horizontal grid. The model used Range–Kutta time integration schemes from the second and third orders and schemes from the second through sixth orders for advection in vertical and horizontal directions (Skamarock et al. 2008).

Weather research and forecasting (WRF) is a mesoscale numerical weather forecasting model designed to forecast weather and satisfy atmospheric research needs. Application of the WRF model is concentrated on simulators with a resolution ranging between one and ten kilometers, although it can be employed in lower resolutions as well. This model allows the researchers to perform simulations both reflecting real data and comprising ideal conditions. Forecasts made by this model are extremely flexible and the resulting calculations are efficient. As shown in Fig. 4, the model is made up of various components and takes advantage of advanced numerical and physical options (Skamarock et al. 2008).

HEC-HMS model introduction

The HEC-HMS hydrologic modeling system was developed by American military engineers and has since replaced the HEC-1 software. This model is concerned with rainfall–runoff simulation (Abbasi et al. 2010). The software is a product of a hydrological engineering research and development program in the civil engineering discipline, is considered a significant achievement in hydrology engineering and computer sciences, and has more flood trending and simulation features compared to the HEC-1 software. Features such as snow melting simulation (Goodarzi et al. 2022), dam failure, reservoir outlet structures, and flood return periods are currently under investigation to be included in the HEC-HMS software but have yet to be finalized. The analysis of the damage caused by floods does not fit into the scope of the HEC-1 model and is separately investigated in HEC-FDA. Moreover, this software includes several new and vital features absent in HEC-1, including continuous flood hydrograph simulation over the long term and distributed flow calculation by mapping the simulated cellular grid in the catchment (Kaffas and Hrissanthou 2014).

The HEC-HMS hydrological modeling system is designed to simulate the rainfall–runoff process in catchment systems. By design, this model is applied in vast geographical areas to address a wide range of problems including water and hydrology in large catchments and floods in small urban or natural watersheds. The model also had a wide range of applications in many regions of the world given the diversity of its sub-models as shown in Fig. 5 (Shokri et al. 2012).

WRF Modeling System Flow Chart

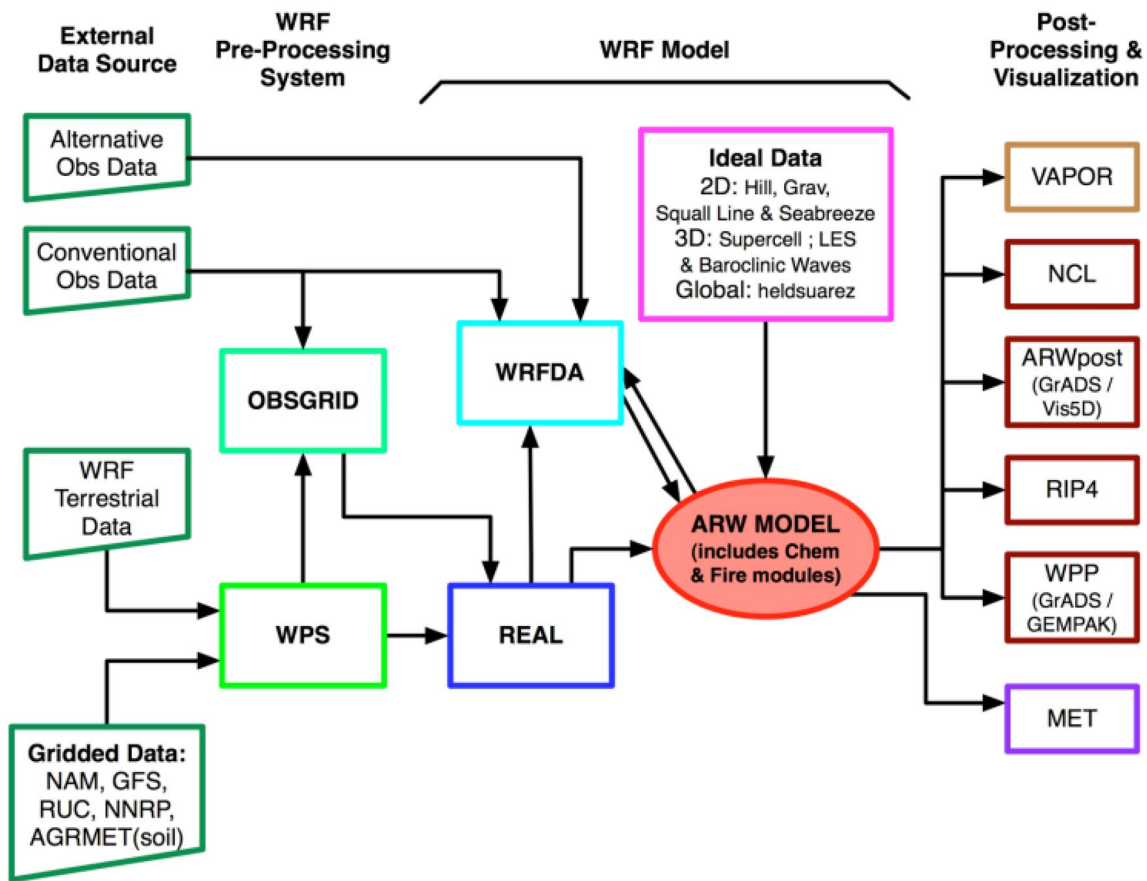


Fig. 4 The main components of the WRF model (WRF 2012)

HEC-HMS model components

Various parameters of the catchment such as loss parameters, curve number, and time of concentration must first be entered into the HEC-HMS model to implement the model (Custódio and Ghisi 2023).

Loss model Loss models generally calculate the runoff volume based on the volume of lost water and its deduction from the rainfall. Although HEC-HMS features various options to model loss, the present study employed the soil conservation service (SCS) curve loss because of its versatility, quantitative input data, a wide range of runoff estimation, and reliable results (Askar 2013), (Lal et al. 2017), (Soulis 2021), (Uwizeyimana et al. 2019).

$$S = \frac{25400}{CN} - 254\text{mm} \tag{1}$$

Transform model Lag time (TL) is the only input parameter for this model, which in turn depends on the time of con-

centration (TC). Lag time and time of concentration are the two parameters determining the speed at which a watershed reacts to precipitation (Sultan et al. 2022).

$$T_c = \left(\frac{L}{1.5D}\right) \left(\sqrt[5]{\frac{A^2}{s}}\right) \tag{2}$$

$$D = 2\sqrt{\frac{A}{\pi}} \tag{3}$$

$$T_l = 0.6 * T_c \tag{4}$$

TL is the lag time (hour); Tc is a time of concentration (hour); L = main channel length (km); A = area in km²; Sc = main channel slope.

Curve number To calculate the curve number, the parameters of land use type and soil hydrological group, and moisture class were first determined using the soil type and land use maps of the region developed in GIS, and the curve number

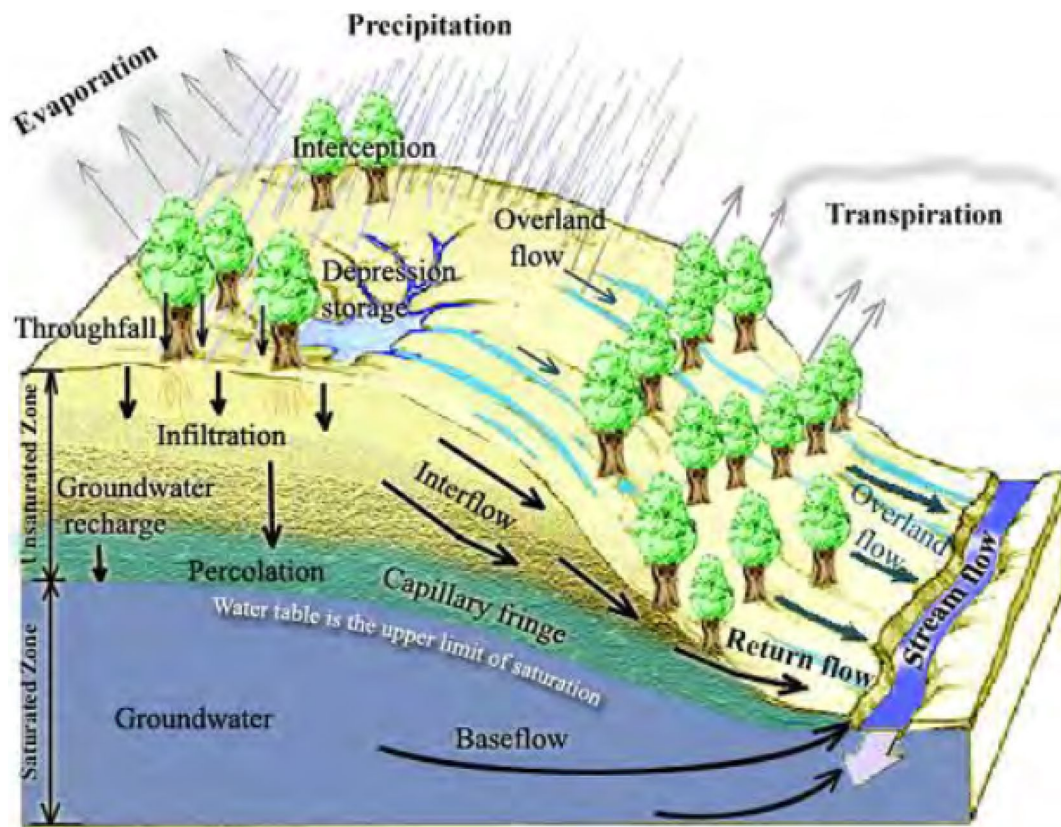


Fig. 5 Physical processes involved in runoff generation (Tarboton 2003)

was eventually determined using the respective tables and the weighted averaging method (Lal et al. 2017).

Error indices

The error indices of root mean square error (RMSE), percent bias (PBIAS), mean absolute error (MAE), and R2 were used to validate the HEC-HMS and WRF models and estimate the output errors of the WRF model, rain gauge station data, HEC-HMS model, and hydrometer station data (Niazkar et al. 2019).

$$RMSE = \sqrt{\frac{\sum_{i=1}^n (O_i^{obs} - O_i^{sim})^2}{n}} \tag{5}$$

$$PBIAS = \sqrt{\frac{\sum_{i=1}^n (O_i^{obs} - O_i^{sim}) * 100}{\sum_{i=1}^n O_i^{obs}}} \tag{6}$$

$$MAE = \frac{\sum_{i=1}^n |O_i^{obs} - O_i^{sim}|}{n} \tag{7}$$

$$R^2 = 1 - \frac{\sum_{i=1}^n (O_i^{sim} - O_i^{obs})^2}{\sum_{i=1}^n (O_i^{obs} - \bar{O}_i)^2} \tag{8}$$

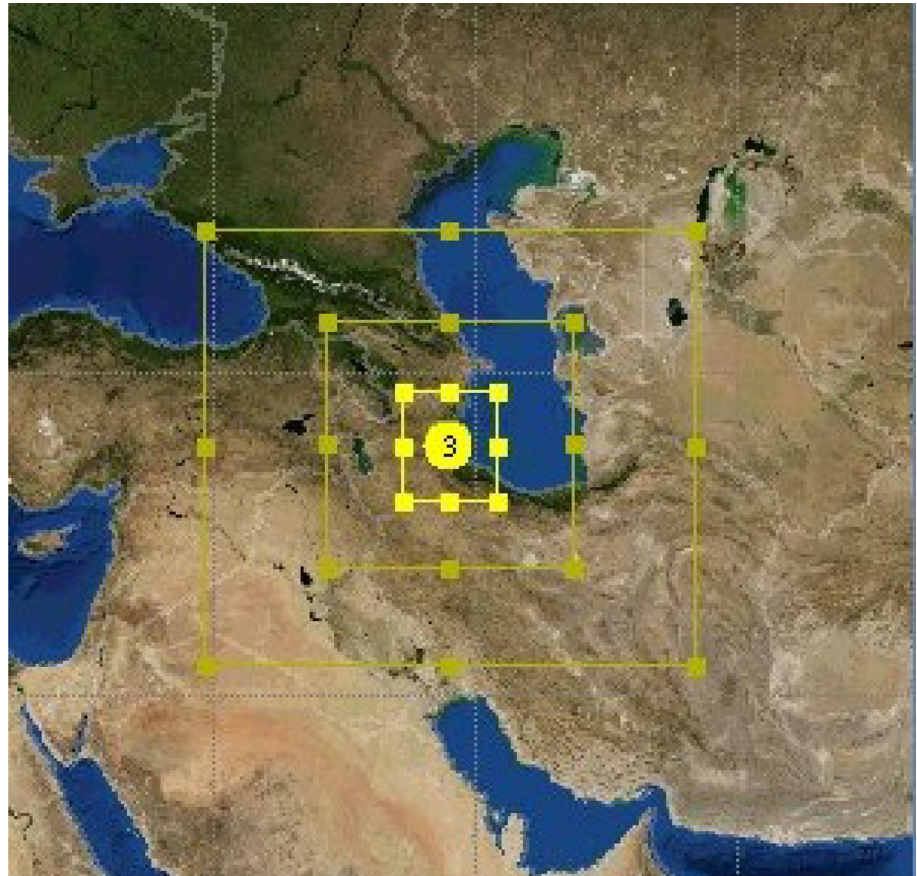
Results

The present section is concerned with how the models were implemented, how WRF and HEC-HMS models were integrated, and the results of data statistical analysis. Therefore, this section first provides an account of each model's calibration and implementation and proceeds to report the results of each model separately.

WRF Model implementation

To implement the WRF model, three domains with vertical and horizontal resolutions of 27, nine, and three kilometers were defined in the first to third domains, respectively, and WRF domain wizard was employed to configure the domains (Fig. 6).

Fig. 6 Configuration of the WRF model domains



WRF model Calibration

The WRF model is composed of various schemes and uses a specific combination of schemes based on the requirements of the task and studied region. Overall, cumulus schemes are more influential in WRF rainfall parameter simulation compared to the other schemes (Patel et al. 2019). Therefore, given the wide range of the schemes, the long time the model requires to run, and the greater sensitivity of cumulus schemes compared to other schemes, Purdue Lin microphysics schemes, MYJ boundary layer scheme, RRTM, and Dudhia Shortwave Scheme short and long wave radiation,

and Eta Similarity Scheme land surface settings were used to estimate the precipitation parameter and even the evaluation of satellite-based products to estimate precipitation for the sustainable management of water resources, which is critical (Goodarzi et al. 2022). A close investigation of the outputs was then performed to find the best cumulus schemes among Kain-Fritsch, Moisture-advection-based Trigger for Kain-Fritsch Cumulus, and Grell 3D Ensemble Schemes to find the fittest answer possible for Talesh watershed precipitations.

Figures 7, 8 and 9 demonstrate the charts on observational data from Talesh station and Kain-Fritsch Cumulus, Kain-Fritsch, and Grell 3D Ensemble schemes drawn using

Fig. 7 Comparison of observational and model's forecasted precipitations from 28.09.2021 to 30.09.2021

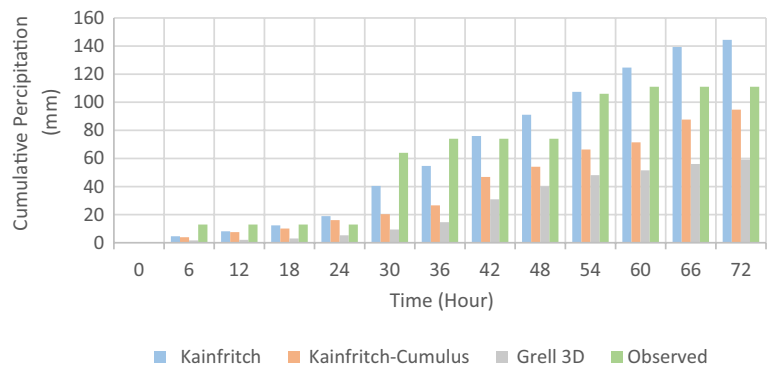


Fig. 8 Comparison of observational and model's forecasted precipitations from 06.10.2021 to 08.10.2021

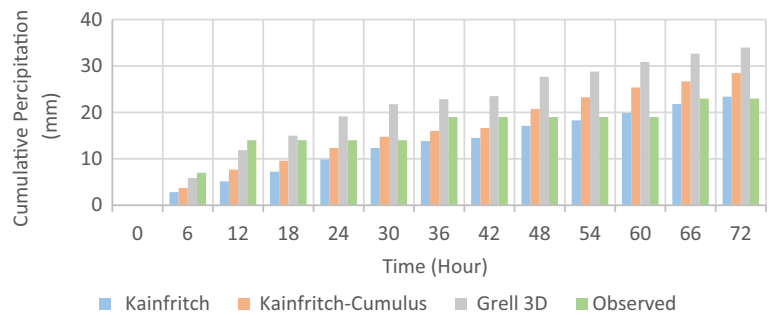
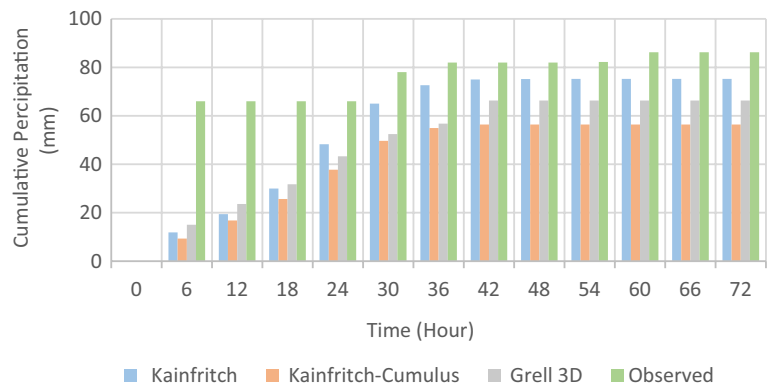


Fig. 9 Comparison of observational and model's forecasted precipitations from 10.11.2021 to 12.11.2021



the WRF model. Each scheme is examined and defined separately in the following to reach a conclusion.

As shown in Figs. 7, 8 and 9 in all three events, the diagram related to the Kain-Fritsch scheme is more similar to the diagram of observation data than other schemes, and the diagram of the Grell 3D scheme is the least similar to has shown itself.

In Fig. 8, the overall trend and value of the actual observed data are most consistent with the results predicted by the second scenario, which is different from Figs. 7 and 9 and needs to be explained. In general, as fine particles in the atmosphere cause the process of precipitation, and the stronger the presence of fine particles, we will see stronger precipitation, but due to the sensitivity to some patterns, sometimes the increase of fine particles gives the opposite result and causes remaining moisture in the upper layers of the atmosphere and forecasting is modeled.

Results of this experiment revealed that the Kain-Fritsch scheme performed the best with a mean RMSE of 9.1, followed by the Kain-Fritsch Cumulus and Grell 3D Ensemble schemes with RMSEs of 11 and 12.2, respectively. Figures 7, 8 and 9 illustrate the aforementioned (Fig. 10) (Table 2).

Comparison of data from the WRF model and rain gauge stations

Figure 11 demonstrates WRF model forecasts versus data from rain gauge stations. Statistical indices of RMSE,

PBIAS, and MAE were used to compare the data from the WRF model and rain gauge stations, yielding the figures of 16.78, 0.9, and 8.68, respectively.

An overview of the results reveals that the model indicated a good performance in simulating the catchment except for two instances of peak rainfall forecast in the first 15 days and the peak at day 60 (the next section will elaborate on the reasons behind estimation errors made in the case of these three peak rainfalls). Another tangible point was the presence of time lags between the rain gauge station and WRF model output data, which can be justified by other forecasting models such as other models and satellite techniques. This also suggests the relatively better performance of this model in forecasting a rainfall system compared to predictions made for rainfall on a specific day.

Analysis of rainfall spatial distribution in Talesh Basin based on the WRF model

To perform a rainfall spatial distribution analysis, three rainfall peak samples obtained from WRF model outputs were examined. Figures 12 and 14 demonstrate that rainfall distribution was more focused on the upstream of the studied river in the first and ninth rainfall peaks, which could be due to the more intense precipitation in the rain gauge station compared to rainfall in the WRF model output. The reason for this is that the rainfall from the WRF model is the average of rainfall cells in the watershed, whereas observational

Fig. 10 RMSE index in precipitation forecasts made by various WRF schemes and observational data

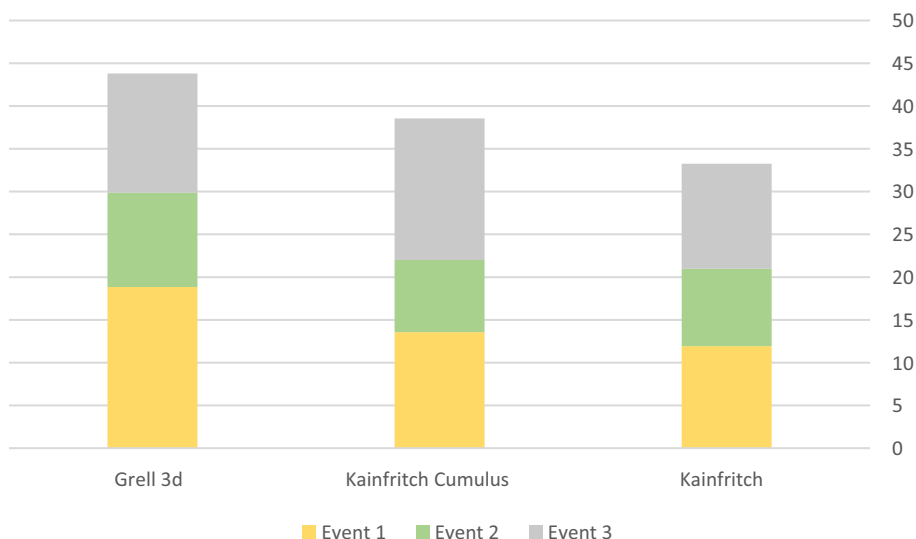


Table 2 Selected WRF model schemes to use in the Talesh catchment

Tier	Physics Scheme	Physics Scheme Symbol	Type of the scheme that used in WRF run
1	Microphysics	mp_physics	<i>Eta Similarity</i>
2	Shortwave and longwave radiation	ra_sw_physics & ra_lw_physics	Dudhia & RRTM
3	Planetary Boundary layer	bl_pbl_physics	MYJ
4	Surface layer	sf_sfclay_physics	Eta Similarity Scheme
5	Cumulus parameterization	cu_physics	Kain – Fritsch for Kain-Fritsch Cumulus Grell 3D Ensemble

Fig. 11 Results from the WRF model and the rain gauge station

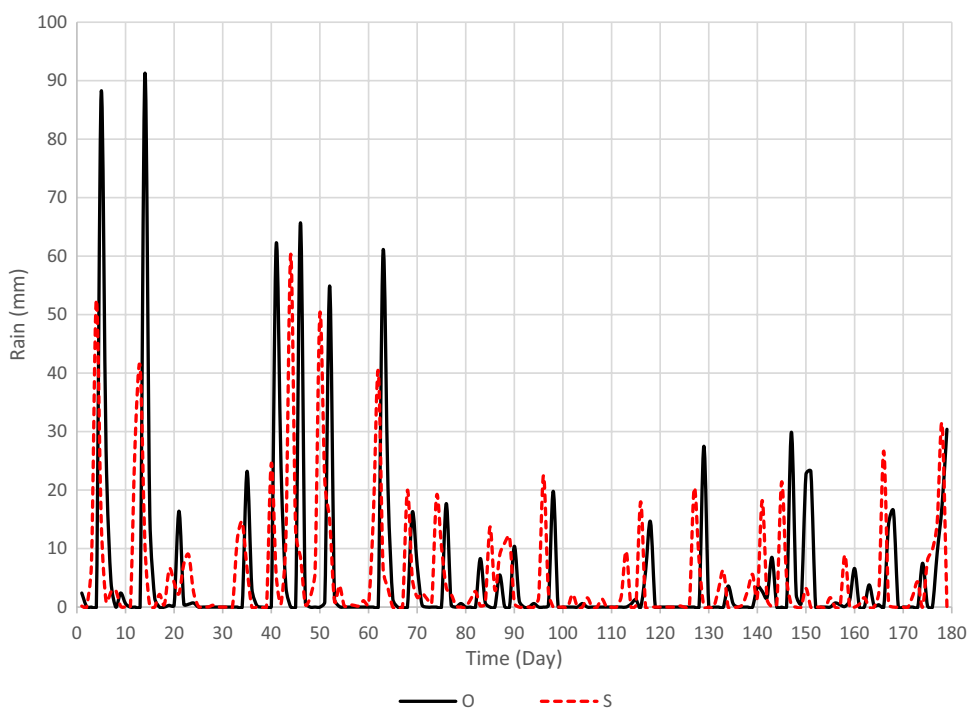


Fig. 12 Spatial distribution of rainfall in the first peak, 09/26/2018

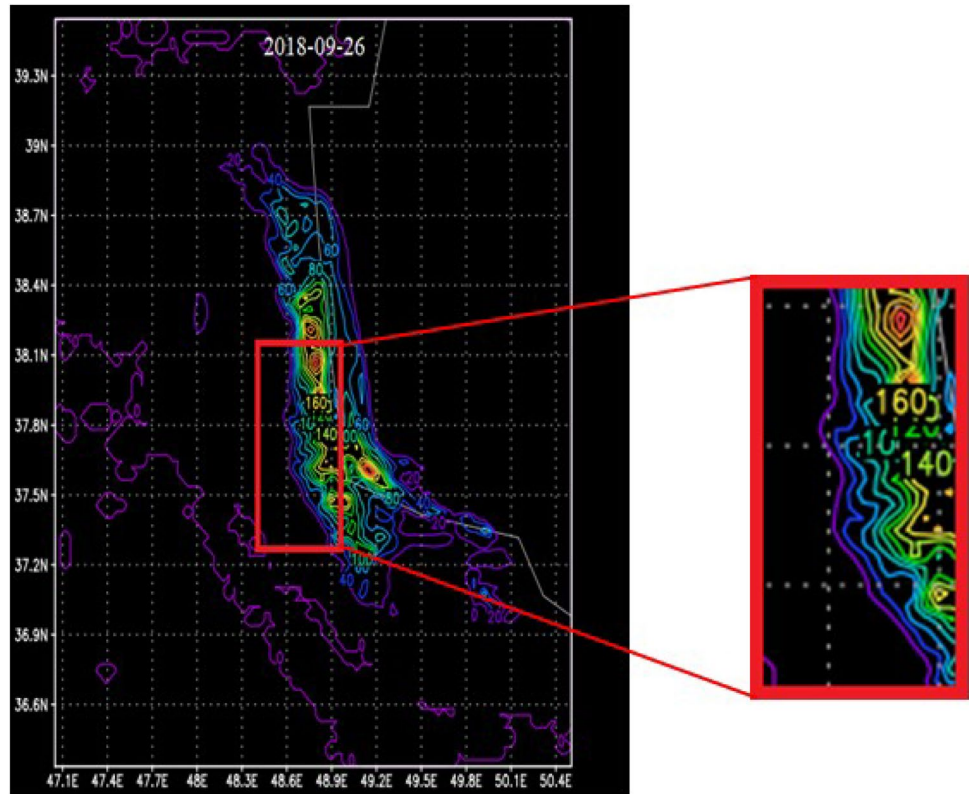
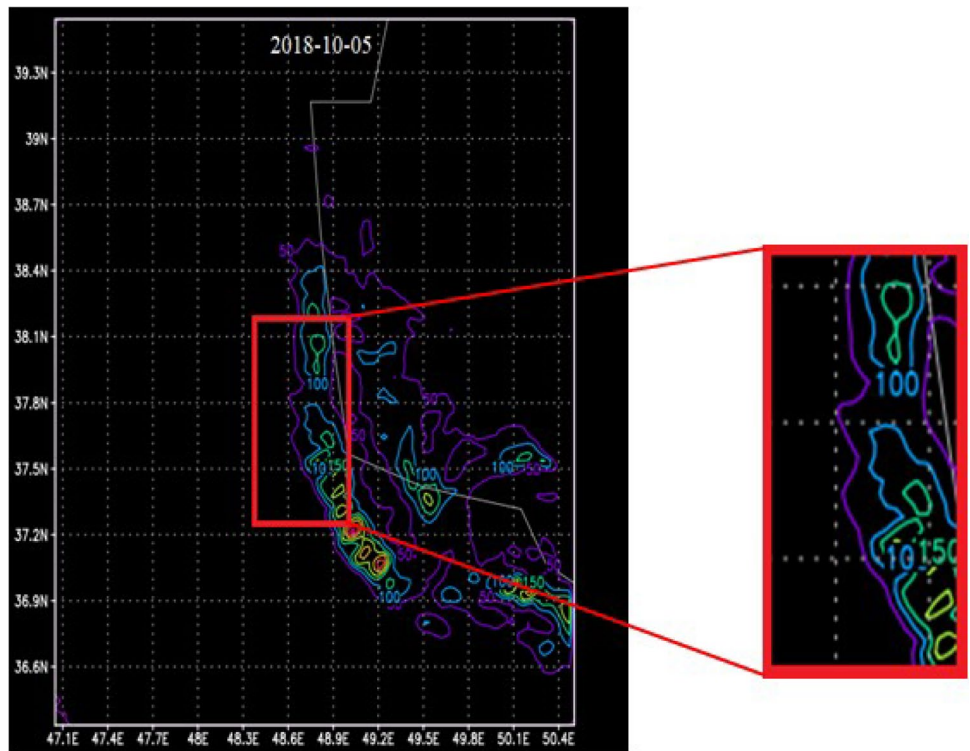


Fig. 13 Spatial distribution of rainfall in the Second peak, 05/10/2018



rain was the point precipitation in the rain gauge station in the proximity of the studied river. Moreover, conditions similar to the first rainfall peak were observed in the second peak as Fig. 13 demonstrates, with the exception that the precipitation was focused on two points over the studied river and the south of the watershed. One could thus suggest that the rainfall in the upstream area of the watershed and the studied river was more than the mean precipitation in the catchment. The reason behind the difference between data observed in the rain gauge station and WRF model output can thus be traced to the difference between mean rainfall in the watershed and the rainfall upstream—and specifically over the studied river—given the aforementioned spatial distribution analysis of the precipitation (Fig. 14).

HEC-HMS model calibration

The calibration process reduced the CN parameter by 20% from 70 to 55 and increased the lag time parameter by 20% from 488 to 585 min.

Figure 15 indicates the observed and forecasted hydrograph for the six months of 09/23/2018 to 03/23/2019. Comparison of the HEC-HMS model output data was performed to observational data using the statistical indices of RMSE, PBIAS, MAE, and R², which were revealed to be 3.41, 0.23, 2.18, 70% and 3.92, 4.9, 2.95, and 87% for volumetric discharge and peak discharge, respectively (Fig. 16). Results thus revealed the appropriate performance of the model. The

tangible point throughout the calibration process was the model's sensitivity to the parameters of CN and lag time, so land permeability would reduce with the increase in CN, resulting in the production of more runoff in the model. Furthermore, the parameter of slope played a prominent part in flood estimation in the studied area as an increased slope would reduce lag time, resulting in a larger runoff volume estimation by the model (Fig. 17).

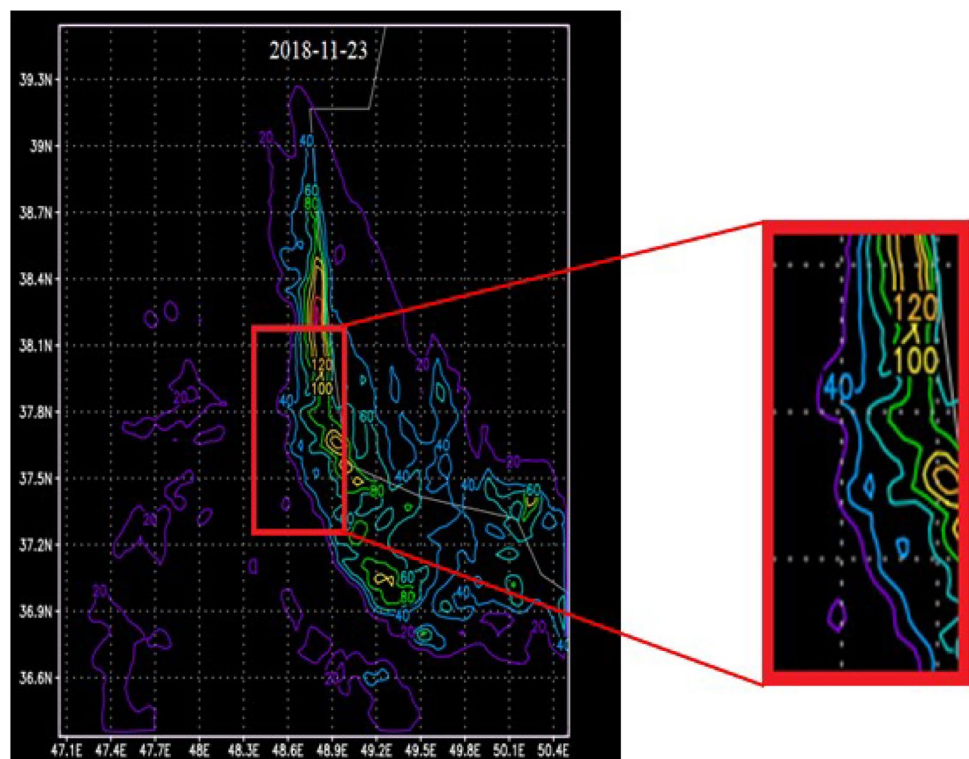
Validating the HEC-HMS model

Model validation is concerned with examining the extent to which the model accurately represents the real system or its intellectual equivalent. Data from the rain gauge and hydrometer over 80 days between 01/01/2018 and 03/20/2018 were used to validate the HEC-HMS model. Results of RMSE, PBIAS, MAE, and R² statistical indices for this period were 1.1, 8.9, 0.8, 83% and 1.2, 7.29, 1.02, and 97% for volumetric and peak discharge, respectively, which revealed the precise calibration of the model (Fig. 18).

Results of the HEC-HMS model coupled with WRF

Figure 19 demonstrates the observational and forecasted hydrographs of the model for the six months between 09/23/2018 and 03/23/2019. As mentioned in Sect. 3.3, this figure indicates the underestimations made in the first, second, and ninth peaks explained in Sect. 3.4. Another notable

Fig. 14 Spatial distribution of rainfall in the ninth peak, 11/23/2018



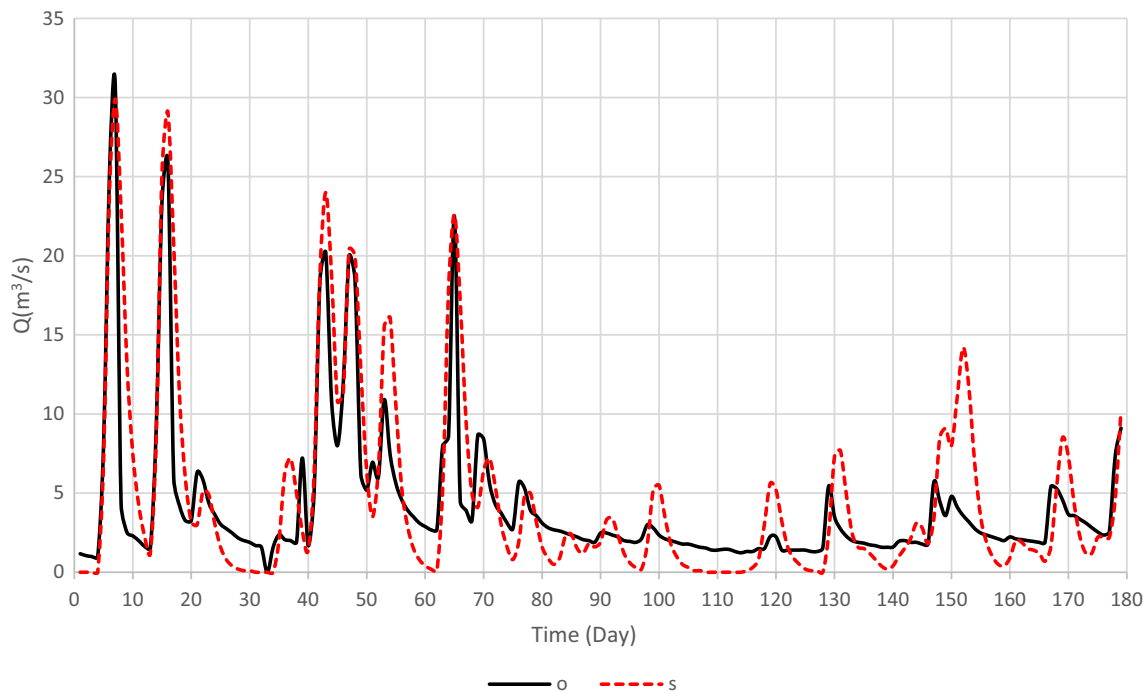
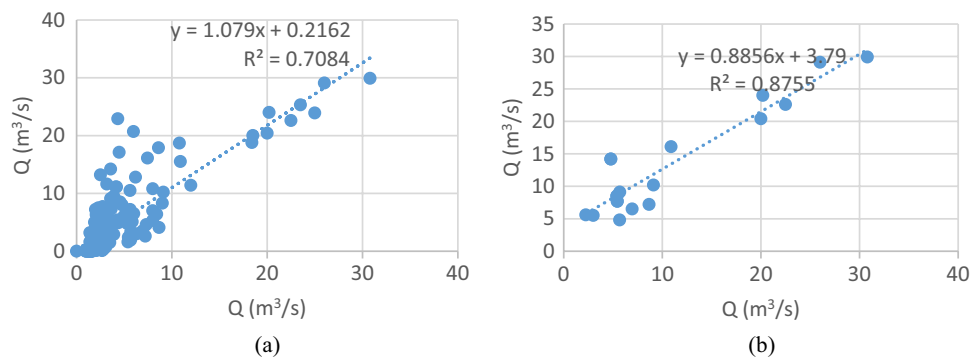


Fig. 15 Comparison of output data from the calibrated HEC-HMS model and observational data

Fig. 16 Results of flood volumetric **a** flood peak **b** discharge evaluation in HEC-HMS model calibration



point was the time lag in forecasting some systems –specifically flood peaks, which was expectable given the nature of the weather forecasting methods. This suggests that WRF and HEC-HMS models were considerably more capable of forecasting the volume of flood in a flood system accurately when combined compared to daily forecasts. Moreover, a significant portion of the time the model was implemented (days 30–60 and day 65 until the end of the period), which includes 80% of the studied period, the runoff predicted by the model exceeded the runoff observed in the hydrometer station in peak flood points. Given the account given in Sect. 3.4 regarding the first, second, and ninth peaks, it could be suggested that the coupled model suffered a general overestimation in peak flood points. However, charts of observational hydrometer station data and integrated WRF

and HEC-HMS model output data were significantly similar over the entire studied time. Finally, the statistical indices of RMSE, PBIAS, and MAE were used to compare the model's output data, which were revealed to be 4.13, 3.42, 2.67 and 6.2, 2.46, and 5.11 for volumetric discharge and peak discharge, respectively.

The consistency of which with the model developed by integrating WRF and HEC-HMS at this date (Fig. 19) indicates the models' capability in simulating flood in Talesh catchment.

Overall, the results indicated that the fact that a vast area of the catchment is geologically made of rocks has increased the volume of runoff, resulting in a high flow discharge in the catchment outlet. On the other hand, the presence of agricultural lands across the catchment outlet highlighted

Fig. 17 HEC-HMS model Validation

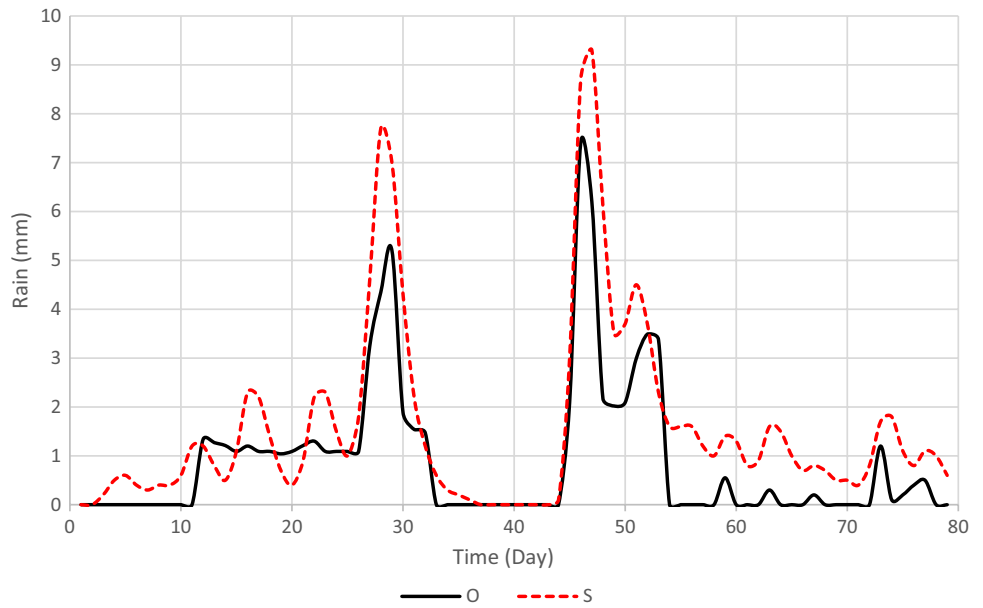


Fig. 18 Results of flood volumetric **a** flood peak **b** discharge evaluation in HEC-HMS model validation

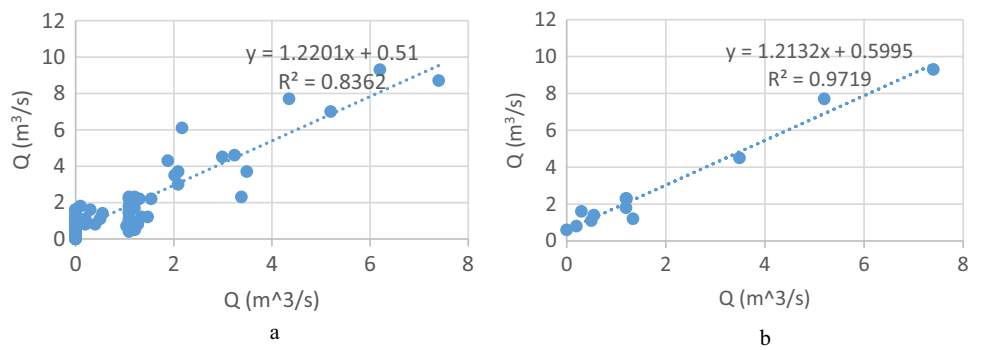
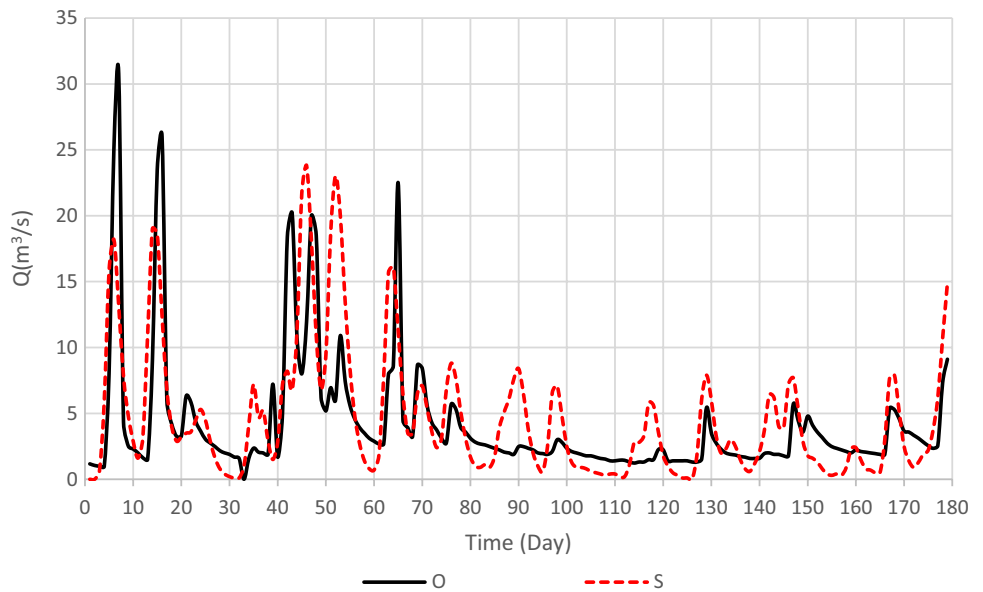


Fig. 19 Comparison of the output data of HEC-HMS model coupled with WRF and observational data



the significance of runoff forecasting in this region as it left crucial impacts on agriculture in the region (rice farming is the dominant form of agriculture in the region) alongside its influence on residential areas. Hence, flood prediction in the region could help develop a disciplined plan for farmers in the area to achieve the best crop yield and mitigate damages in the case that a flood is predicted. The WRF model is thus recommended to be integrated with the hydrological model in predicting flood when developing and compiling flood warning systems in flood-prone regions of the country (Goudarzi et al. 2018).

Conclusion

Flood warnings are crucial in saving lives and properties from natural disasters. Therefore, providing evacuation information to flood-prone plains by giving clear warnings would prove tangibly beneficial and mitigate damages caused by disasters significantly. Cooperation between governments, local communities, and regional weather and water departments would be essential in accomplishing this goal. Increased awareness and improved preparedness are among the essential factors in making the unstructured measures mentioned in the present study more efficient.

The present study employed the WRF v.4.1 weather research and forecasting model to forecast rainfall in a watershed. 48-h implementation periods were considered for this purpose as the first 24 h was considered to minimize initial model errors and the next 24 h were considered as the final output of the model. Results indicated the RMSE, PBIAS and MAE statistical indices of 16.78, 0.9, and 8.68, respectively, revealing the good performance of the model in forecasting rainfall in the studied region compared to precipitation data from a rain gauge station. Moreover, a comparison of 24-h forecasts to forecasts made over longer periods indicated that 24-h forecasts were more accurate in the WRF model. Besides, results indicated that constant implementation of the HEC-HMS model resulted in a suitable flood forecasting performance. To calibrate the HEC-HMS model, a sensitivity analysis was performed, indicating that the optimized components of curve number (CN) and lag time were the most sensitive. The statistical indices of RMSE, PBIAS, MAE, and R2 were then calculated to be 3.41, 0.23, 2.18, and 70% and 3.92, 4.9, 2.95, and 87% for volumetric discharge and peak discharge, respectively, which indicated the significant similarity between observed and simulated hydrographs. Data from the rain gauge and hydrometer over 80 days between 01/01/2018 and 03/20/2018 were used to validate the HEC-HMS model. Results of RMSE, PBIAS, MAE, and R2 statistical indices for this period were 1.1, 8.9, 0.8, 83%, and 1.2, 7.29, 1.02, and 97% for volumetric and peak discharge, respectively. Ultimately, RMSE, PBIAS, and

MAE were calculated to examine the flood forecasting performance by the coupled model in the studied region, which was revealed to be 4.13, 3.42, and 2.67 for volume flow and 6.2, 2.46, and 5.11 for peak flow, suggesting the model's acceptable performance in Talesh catchment.

Funding The authors received no specific funding for this work.

Declarations

Conflict of interest The authors declare that they have no known competing financial interests or personal relationships that could have appeared to influence the work reported in this paper.

Open Access This article is licensed under a Creative Commons Attribution 4.0 International License, which permits use, sharing, adaptation, distribution and reproduction in any medium or format, as long as you give appropriate credit to the original author(s) and the source, provide a link to the Creative Commons licence, and indicate if changes were made. The images or other third party material in this article are included in the article's Creative Commons licence, unless indicated otherwise in a credit line to the material. If material is not included in the article's Creative Commons licence and your intended use is not permitted by statutory regulation or exceeds the permitted use, you will need to obtain permission directly from the copyright holder. To view a copy of this licence, visit <http://creativecommons.org/licenses/by/4.0/>.

References

- Abbasi M, Mohseni Saravi M, Kheirkhah MM, Sigaroudi Sh Khalighi, Gh Rostamizad M, Hosseini, (2010) Assessment of Watershed Management Activities on Time of Concentration and Curve Number using HEC-HMS Model (Case Study: Kan Watershed, Tehran). *J Range Watershed Manag* 63(3):375–385 (https://jrwms.ut.ac.ir/article_22871.html?lang=en)
- Anderson ML et al (2002) Coupling HEC-HMS with atmospheric models for prediction of watershed runoff. *J Hydrol Eng* 7(4):312–318. [https://doi.org/10.1061/\(ASCE\)1084-0699\(2002\)7:4\(312\)](https://doi.org/10.1061/(ASCE)1084-0699(2002)7:4(312))
- Askar MK (2013) Rainfall-runoff model using the SCS-CN method and geographic information systems: a case study of Gomal River watershed. *WIT Trans Ecol Environ* 178:159–170. <https://doi.org/10.2495/WS130141>
- Custódio DA, Ghisi E (2023) Impact of residential rainwater harvesting on stormwater runoff. *J Environ Manag* 326:116814. <https://doi.org/10.1016/j.jenvman.2022.116814>
- Tarboton DG (2003) Rainfall-runoff processes. A workbook to accompany the rainfall-runoff processes web module. Utah State University. <https://hydrology.usu.edu/rrip/>, <https://hydrology.usu.edu/rrip/pdfs/RainfallRunoffProcesses.pdf>
- Goodarzi MR, Vazirian M (2023) A geostatistical approach to estimate flow duration curve parameters in ungauged basins. *Appl Water Sci* 13(9):178. <https://doi.org/10.1007/s13201-023-01993-4>
- Goodarzi MR et al (2022) Urban WEF Nexus: an approach for the use of internal resources under climate change. *Hydrology* 9(10):176. <https://doi.org/10.3390/hydrology9100176>
- Goodarzi MR, Pooladi R, Niazkar M (2022) Evaluation of satellite-based and reanalysis precipitation datasets with gauge-observed data over Haraz-Gharehsoo Basin, Iran. *Sustainability* 14(20):13051. <https://doi.org/10.3390/su142013051>
- Goodarzi MR, Sabaghzadeh M, Mokhtari MH (2022) Impacts of aspect on snow characteristics using remote sensing from 2000 to 2020

- in Ajichai-Iran. *Cold Regions Sci Technol* 204:103682. <https://doi.org/10.1016/j.coldregions.2022.103682>
- Gore JA, Petts GE (eds) (1989) *Alternatives in regulated river management*. Fla CRC Press, Boca Raton (<https://westminsterresearch.westminster.ac.uk/item/94w15/alternatives-in-regulated-river-management>)
- Goudarzi L, Banihabib ME, Ghafarian P (2018) Evaluation of the WRF model performance for heavy rainfall simulation a case study of the Kan Basin in Iran. *J Water Soil Conserv* 25(1):229–242. <https://doi.org/10.22069/JWSC.2018.11669.2613>
- Kaffas K, Hrissanthou V (2014) Application of a continuous Rainfall-Runoff model to the basin of Kosynthos river using the hydrological software HEC-HMS. *Global NEST J* 16(1):188–203. <https://doi.org/10.30955/gnj.001200>
- Kaya CM, Derin L (2023) Parameters and methods used in flood susceptibility mapping: a review. *J Water Clim Change* 14(6):1935–1960. <https://doi.org/10.2166/wcc.2023.035>
- Lal M et al (2017) Evaluation of the soil conservation service curve number methodology using data from agricultural plots. *Hydrogeol J* 25(1):151–167. <https://doi.org/10.1007/s10040-016-1460-5>
- McQueen J, Draxler R, Stunder B (1997) Applications of the regional atmospheric modeling system (RAMS) at the NOAA air resources laboratory, in. Available at: <https://nla.gov.au/nla.cat-vn4126870>
- Merino A et al (2022) WRF hourly evaluation for extreme precipitation events. *Atmos Res* 274:106215. <https://doi.org/10.1016/j.atmosres.2022.106215>
- Nasiri Z, Talebi A (2020) Prioritization of sub-watersheds from flooding viewpoint using the Hec-Hms model in upstream of Shiraz Khoshk River. *Iran J Ecohydrol*. <https://doi.org/10.22059/IJE.2020.284092.1145> (https://ije.ut.ac.ir/article_75819.html?lang=en)
- Niazkar M, Talebbeydokhti N, Afzali SH (2019) One dimensional hydraulic flow routing incorporating a variable grain roughness coefficient. *Water Resour Manag* 33(13):4599–4620. <https://doi.org/10.1007/s11269-019-02384-8>
- Patel P et al (2019) Performance evaluation of WRF for extreme flood forecasts in a coastal urban environment. *Atmos Res* 223:39–48. <https://doi.org/10.1016/j.atmosres.2019.03.005>
- Pleim JE, Gilliam R (2009) An indirect data assimilation scheme for deep soil temperature in the Pleim-Xiu land surface model. *J Appl Meteorol Climatol* 48(7):1362–1376. <https://doi.org/10.1175/2009JAMC2053.1>
- Roy D et al (2013) Calibration and validation of HEC-HMS model for a river basin in Eastern India. *ARPN J Eng Appl Sci* 8(1):40–56
- Shokri S et al (2012) Watershed flood hydrograph estimation using HEC-HMS and geographic information system (case study: idanak watershed). *JWMR* 3(5):63–80
- Singh A et al (2021) A review of modelling methodologies for flood source area (FSA) identification. *Nat Hazards* 107(2):1047–1068. <https://doi.org/10.1007/s11069-021-04672-2>
- Skamarock WC et al. (2008) A Description of the advanced research wrf version 3. NCAR Technical Notes [Preprint]. Available at: <https://doi.org/10.5065/D68S4MVH>
- Soulis KX (2021) Soil conservation service curve number (SCS-CN) method: current applications, remaining challenges, and future perspectives. *Water* 13(2):192. <https://doi.org/10.3390/w13020192>
- Sultan D et al (2022) Evaluation of lag time and time of concentration estimation methods in small tropical watersheds in Ethiopia. *J Hydrol Region Stud* 40:101025. <https://doi.org/10.1016/j.ejrh.2022.101025>
- Tedla HZ et al (2022) ‘Evaluation of WRF model rainfall forecast using citizen science in a data-scarce urban catchment: Addis Ababa, Ethiopia. *J Hydrol Region Stud* 44:101273. <https://doi.org/10.1016/j.ejrh.2022.101273>
- Uwizeyimana D et al (2019) ‘Modelling surface runoff using the soil conservation service-curve number method in a drought prone agro-ecological zone in Rwanda. *Int Soil Water Conserv Res* 7(1):9–17. <https://doi.org/10.1016/j.iswcr.2018.12.001>
- WRF Modeling System Overview Wei Wang and Jimy Dudhia University of Sao Paulo, Brazil October 16, 2012. https://ruc.noaa.gov/wrf/wrf-chem/wrf_tutorial_2012_brazil/WRF_overview.pdf
- Weisman ML et al (2008) Experiences with 0–36-h explicit convective forecasts with the WRF-ARW model. *Weather Forecast* 23(3):407–437. <https://doi.org/10.1175/2007WAF2007005.1>
- Zhang C, Wang Y, Hamilton K (2011) Improved representation of boundary layer clouds over the southeast Pacific in ARW-WRF using a modified tiedtke cumulus parameterization scheme. *Mon Weather Rev* 139:3489–3513. <https://doi.org/10.1175/MWR-D-10-05091.1>

Publisher's note Springer Nature remains neutral with regard to jurisdictional claims in published maps and institutional affiliations.